Available online at BCREC Website: http://bcrec.undip.ac.id

Bulletin of Chemical Reaction Engineering & Catalysis, 12 (2), 2017, 206-211

Research Article

Synthesis of Ag_3PO_4 using Hydrophylic Polymer and Their Photocatalytic Activities under Visible Light Irradiation

Uyi Sulaeman[1]*, Bin Liu[2], Shu Yin[2], Tsugio Sato[2]

[1]*Department of Chemistry, Jenderal Soedirman University, Jl. Dr. Soeparno,*
Purwokerto 53123, Indonesia
[2]*Institute of Multidisciplinary Research for Advanced Materials, Tohoku University,*
Sendai 980-8577, Japan

Received: 13rd November 2016; Revised: 10th February 2017; Accepted: 10th February 2017

Abstract

The highly active Ag_3PO_4 photocatalysts were successfully synthesized using the hydrophylic polymer of PVA (polyvinyl alcohol), PEG (polyethylene glycol) and PVP (polyvinyl pyrrolidone). The products were characterized using X-ray diffraction (XRD), Diffuse reflection spectroscopy (DRS), Field emission scanning electron microscope (FE-SEM), Brunauer–Emmett–Teller (BET) specific surface area, and X-ray photoelectron spectroscopy (XPS). Photocatalytic activities were evaluated using decomposition of Rhodamine B (RhB) under visible light irradiation. The results showed that the PVA, PEG, and PVP increased the specific surface area and enhanced the photocatalytic activity of Ag_3PO_4. The highest photocatalytic activity could be observed in Ag_3PO_4 synthesized with PVA, mainly due to an increase in electron excitation induced by PVA chemically adsorbed on the surface. Copyright © 2017 BCREC Group. All rights reserved

Keywords: Ag_3PO_4; Photocatalyst; Polyvinyl alcohol; Polyethylene glycol; Polyvinyl pyrrolidone

How to Cite: Sulaeman, U., Liu, B., Yin, S., Sato, T. (2017). Synthesis of Ag_3PO_4 using Hydrophylic Polymer and Their Photocatalytic Activities under Visible Light Irradiation. *Bulletin of Chemical Reaction Engineering & Catalysis*, 12 (2): 206-211 (doi:10.9767/bcrec.12.2.767.206-211)

Permalink/DOI: http://dx.doi.org/10.9767/bcrec.12.2.767.206-211

1. Introduction

The wastewater treatment technology is very important for the future to provide an improved environmental health, especially in developing countries where the industries are growing rapidly. The effective method for organic pollutant degradation is a key point in the wastewater treatment. Many researchers have used TiO_2-based photocatalysts for organic pollutant degradation due to high reactivity and stability [1-4]. However, TiO_2 cannot use visible light such as sunlight due to its large band gap energy. TiO_2 can only use UV light irradiation which needs high cost. Therefore, new photocatalyst which has small band gap energy for highly reactive photocatalysis is expected.

Recently, it was reported that silver phosphate has high photocatalytic activity under visible light irradiation due to its lower band gap energy [5-8]. It is a new candidate of photocatalyst which can be applied for wastewater treatment. The improvement of visible light responsive photocatalyst activity of silver phosphate has been investigated by many researchers. It

---

* Corresponding Author.
E-mail: uyi_sulaeman@yahoo.com
Telp.: +62-281-638793; Fax.: +62-281-638793

was reported that the hydrophylic polymer such as polyethylene glycol and polyvinyl pyrrolidone were useful to control the morphology of the photocatalysts. The Ag_3PO_4 porous micro-tubes were successfully prepared by one-pot synthesis using polyethylene glycol 200 (PEG 200) as the reaction medium [7]. This porous material exhibited a higher photocatalytic activity for degradation of RhB. Highly uniform Ag_3PO_4 microspheres with novel 3D flower-like morphology were successfully fabricated through a facile aqueous solution route in the presence of polyethylene glycol [8]. This material enhanced photocatalytic activity of methylene blue (MB) degradation under visible light irradiation. Ag_3PO_4 crystals with various morphologies were successfully synthesized using a facile chemical precipitation method with polyvinyl pyrrolidone (PVP) [9]. The PVP could act as stabilizer for preventing the aggregation of the products and also could act as a shape controller by selective interaction with a specific plane of Ag_3PO_4. With this method, the cubic Ag_3PO_4 particles was found and showed high photocatalytic activity due to the larger surface area and easier separation of hole-electron pairs. The hydrophylic polymer of polyvinyl alcohol (PVA) could also be used to synthesize the Ag_3PO_4/PVA microcrystal hybrid film using a co-precipitation method [10]. The Ag_3PO_4/PVA hybrid showed excellent photocatalytic degradation of RhB under visible light irradiation.

However, the reactivity comparison of Ag_3PO_4 photocatalyst, that synthesized using various hydrophylic polymers, has not been investigated. Therefore, the synthesis of Ag_3PO_4 using hydrophylic polymer of PVA, PEG, and PVP and their photocatalytic activities is very important to obtain the highest reactive photocatalyst under visible light irradiation. This report also presented the deep understanding of photocatalyst using XPS analysis. The new phenomenon of phosphate deficient Ag_3PO_4 was clearly observed and might be a key role for enhancing the interaction of PVA and Ag_3PO_4 in the surface. The PVA chemically adsorbed on the surface might enhance the electron excitation under photoirradiation which improves the photocatalytic activity.

2. Materials and Methods

2.1. Preparation and characterization of photocatalyst

The Ag_3PO_4 photocatalysts were prepared using silver nitrate (Kanto Chemical Co., Inc., 99.7%), sodium phosphate dibasic dodecahydrate (Sigma-Aldrich, 99%) as starting material. The high purity hydrophylic polymer of po-lyvinyl alcohol#500, polyethylene glycol#600 and polyvinyl pyrrolidone k30 were purchased from Kanto Chemical Co., Inc., and used as received. Typically, 1 gram of PVA (polyvinyl alcohol), PEG (polyethylene glycol), PVP (polyvinyl pyrrolidone), 0.0025 mole $AgNO_3$ and 0.0025 mole $Na_2HPO_4.12H_2O$ were dissolved in 100 ml of deionized water separately. After mixing the hydrophylic polymer aqueous solution and $AgNO_3$ aqueous solution under magnetic stirring at 500 rpm, $Na_2HPO_4.12H_2O$ aqueous solution was added slowly and mixed for 30 minutes under magnetic stirring. The precipitates were separated by 14,000 rpm centrifugation. The samples were washed with water and acetone, dried in a vacuum over night at 60 ^{o}C [10].

The crystal structure of the product was characterized using an XRD (Bruker AXS D2 Phaser). The morphologies were investigated using an FE-SEM (Hitachi S-4800). The band gap energies were investigated using UV-Vis DRS (Shimadzu UV-2450), and the specific surface areas were determined by the BET method. The binding energies of samples were investigated using XPS (Perkin Elmer PHI 5600) with Ar^+ sputtering treatment to eliminate the compound adsorbed on the surface before analysis.

2.2. Photocatalytic evaluation

To evaluate the photocatalytic activity, after mixing the 100 ml of Rhodamine B solution (10 mg/L) and 100 mg of catalyst by stirring at room temperature for 20 minutes (under dark condition), the LED blue light (λ = 445 nm) was irradiated, and the solution was withdrawn every 10 minutes, centrifuged at 14,000 rpm to separate the catalyst, then the concentrations of RhB were measured using a spectrophotometer [10,11].

3. Results and Discussion

The XRD patterns of Ag_3PO_4 synthesized with different hydrophylic polymer are shown in Figure 1. It can be seen that the diffraction profiles of Ag_3PO_4 synthesized with PVA, PEG, and PVP are in good agreement with that of the body-centered-cubic structure of Ag_3PO_4 (JCPDS no.06-0505), with the space group of p-43n. There are no impurities observed in XRD patterns.

Figure 2 showed the DRS of Ag_3PO_4 synthesized with different hydrophylic polymer of PVA, PEG, and PVP. The broad absorption could be observed in the spectra of Ag_3PO_4 synthesized using PVA and PVP, and the highest broad absorption above 500 nm was found in Ag_3PO_4 synthesized with PVA. The Ag_3PO_4 synthesized using PEG showed the absorption band edge shift to the lower wavelength (blue shift). The band gaps of the samples were calculated from the DRS using the equation of direct transition semiconductor [10,12] as presented in Equation (1):

$$\alpha h\nu = A(h\nu - E_g)^{n/2} \quad (1)$$

where *α, ν, E_g,* and *A* are absorption coefficient, light frequency, band gap energy, and a constant, respectively. The band gap of 2.35, 2.32, 2.37, and 2.35 eV could be observed in Ag_3PO_4, Ag_3PO_4/PVA, Ag_3PO_4/PEG, and Ag3PO4/PVP, respectively (Table 1).

Figure 3 shows the morphology of Ag_3PO_4 synthesized without and with hydrophylic polymer of PVA, PEG, and PVP. All samples consisted of the similar spherical particles. The addition of hydrophylic polymers slightly decreased particle sizes, i.e the spherical Ag_3PO_4 exhibited ~200-600 nm in diameter, whereas the spherical Ag_3PO_4/PVA, Ag_3PO_4/PEG, and Ag_3PO_4/PVP exhibited ~150-400 nm in diameter.

Figure 4 shows the photocatalytic activities of Ag_3PO_4 synthesized without and with hydrophylic polymer of PVA, PEG and PVP. The rate constants are evaluated by the following apparent pseudo-first-order kinetics equation [10,12,13] as depicted in Equation (2).

$$\ln \frac{C_0}{C} = k_{app}\, t \quad (2)$$

where *C_0* and *C* are the concentrations of dye in solution at times 0 and *t*, respectively, and k_{app} is the apparent pseudo-first-order rate constant (min^{-1}). The rate constant of 0.021, 0.0312, 0.0278 and 0.0238 could be achieved by Ag_3PO_4, Ag_3PO_4/PVA, Ag_3PO_4/PEG, Ag_3PO_4/PVP, respectively. All of the hydrophylic polymers enhanced the photocatalytic activity of Ag_3PO_4, where the highest photocatalytic activity was observed for Ag_3PO_4 synthesized using PVA. The enhanced photocatalytic activity of Ag_3PO_4 synthesized using PEG and PVP seemed to be caused by increasing the specific surface area. The specific surface area of 3.20 m^2/g was observed in Ag_3PO_4, then increased to 13.2 and 24.2 m^2/g for Ag_3PO_4/PEG and Ag_3PO_4/PVP, respectively. However, the highest photocatalytic activity was observed in Ag_3PO_4/PVA, which did not possess the highest

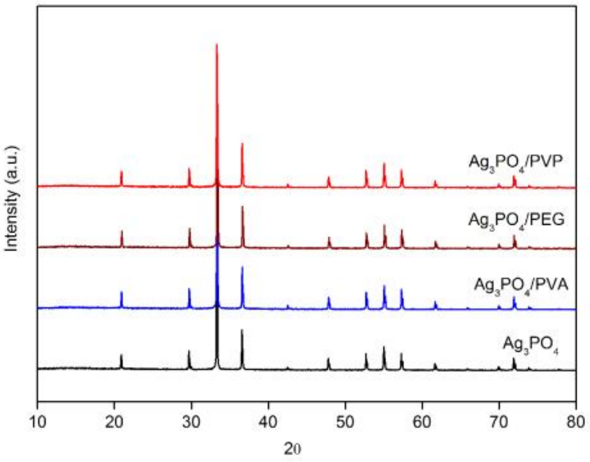

Figure 1. The XRD profiles of Ag_3PO_4, Ag_3PO_4/PVA, Ag_3PO_4/PEG, and Ag_3PO_4/PVP

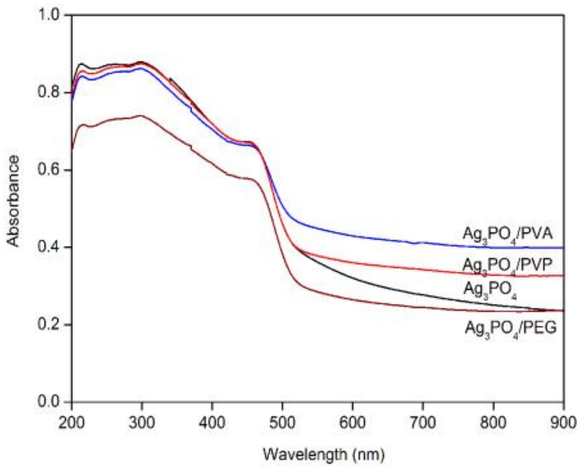

Figure 2. The DRS of Ag_3PO_4, Ag_3PO_4/PVA, Ag_3PO_4/PEG, and Ag_3PO_4/PVP

Table 1. The specific surface areas (S.S.A.), band gap energies and rate constants (*K_{app}*)

Sample	S.S.A. ($m^2 \cdot g^{-1}$)	Band gap energy (eV)	*K_{app}* (min^{-1})
Ag_3PO_4	3.20	2.35	0.0210
Ag_3PO_4/PVA	7.08	2.32	0.0312
Ag_3PO_4/PEG	13.2	2.37	0.0278
Ag_3PO_4/PVP	24.2	2.35	0.0238

specific surface area (7.08 m^2/g), indicating that the high photocatalytic activity of Ag_3PO_4/PVA was caused not only by an increase of the specific surface area but also by unique properties of Ag_3PO_4/PVA.

To understand the unique properties of Ag_3PO_4/PVA, the detailed investigation was conducted by XPS. The binding energy (BE) profiles of Ag_3PO_4 and Ag_3PO_4/PVA is shown in Figure 5. The peak of 133.77 eV can be attributed to binding energy of P^{5+} state [14]. The O1s peak at 531 eV is related to O–Ag bonding, whereas the shoulder peak at higher binding energy is related to OH group [15-16] that might be attributed to the adsorption and dissociation of H_2O on Ag_3PO_4 surface [17]. The shifts of binding energy could be observed in P2p and O1s. The shifts of binding energy indicate that there are different environments of state, which are induced by PVA. The BE of Ag4d was shifted a little toward a higher energy, whereas the BE of P2p and O1s was noticeably shifted to a lower energy, i.e., the BE of P2p were shifted 0.12 eV from 133.77 eV to 133.65 eV and that of O1s was shifted 0.19 eV from 531.0 eV to 530.81 eV. The small amount of the carbon was observed, i.e. 1.19 mass % of carbon atom was identified, indicating that the PVA chemically adsorbed on the surface of Ag_3PO_4. Based on the XPS measurement, with adding PVA, the O/Ag and P/Ag atomic ratio decreased significantly (Table 2), indicating that the deficiency of PO_4^{3-} ion at the surface was formed. The deficiency generates the vacancy site at the surface of Ag_3PO_4, which may be replaced by C–O of PVA. However, the value of C/Ag atomic ratio (C/Ag = 0.029) of Ag_3PO_4/PVA is low compared with the decrease in O/Ag and P/Ag atomic ratios after PVA treatment as shown in Table 2, indicating that the vacancy of PO_4^{3-} is mainly formed at the surface of Ag_3PO_4.

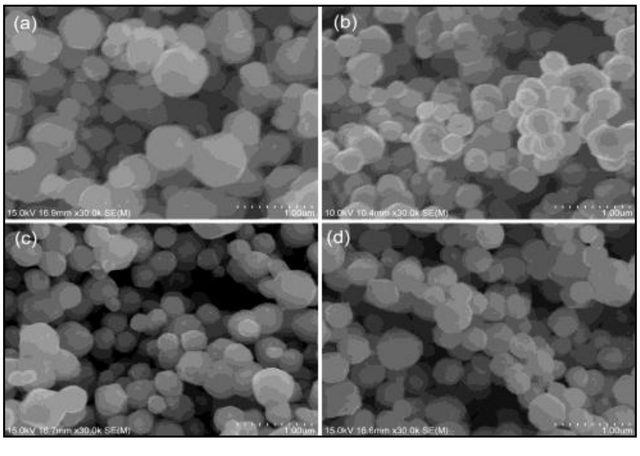

Figure 3. The morphology of Ag_3PO_4 (a), Ag_3PO_4/PVA (b), Ag_3PO_4/PEG (c), and Ag_3PO_4/PVP (d)

The mechanism of the Ag_3PO_4/PVA photocatalyst could be similar with previous reports [10,13]. Under visible light irradiation, the electrons in VB of Ag_3PO_4 could be excited to its CB, leaving hole (+) in VB and electron in CB which is very important for degradation of pollutant. In the same time, the blue light irradiation might generate the excitation of PVA on the surface of Ag_3PO_4 to form the exited PVA (PVA*). The excited electrons in PVA are injected to the conduction band of Ag_3PO_4. The injected electrons migrate to the edge of Ag_3PO_4 and then react with the oxygen (O_2) adsorbed on the surface of Ag_3PO_4 to produce the superoxide radicals ($\bullet O_2^-$), and then form hydroxyl radicals ($\bullet$OH). The superoxide radicals ion $\bullet O_2^-$ and hydroxyl radical $\bullet$OH have the

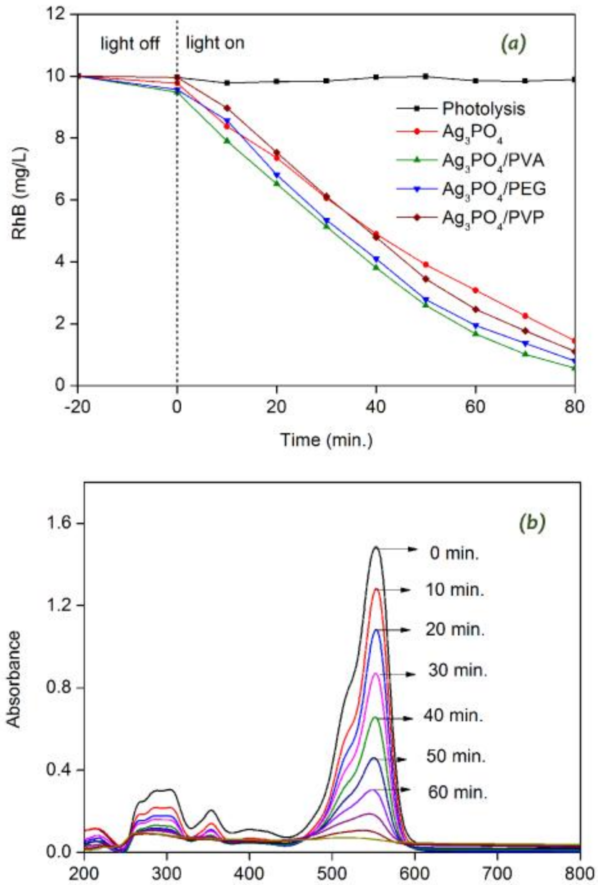

Figure 4. Photocatalytic activity of Ag_3PO_4 synthesized using variation of hydrophylic polymer of PVA, PEG and PVP (a), the UV-Vis absorption spectra of the RhB aqueous solutions vs photocatalytic reaction time (minutes) in the presence of the highest photocatalytic activity of Ag_3PO_4/PVA (b)

important roles for the oxidation of organic compound, such as Rhodamine B. The electrons migrate from the PVA to Ag_3PO_4 surfaces promoted the reaction of photocatalytic activity.

4. Conclusions

The Ag_3PO_4 could be successfully synthesized under hydrophylic polymer of PVA (polyvinyl alcohol), PEG (polyethylene glycol), and PVP (polyvinyl pyrrolidone). The PVA, PEG and PVP increased the specific surface area and enhanced the photocatalytic activity of Ag_3PO_4 under the visible light irradiation. The highest photocatalytic activity could be observed in Ag_3PO_4 synthesized with PVA. The highest photocatalytic activity is mainly due to enhanced electron excitation induced by PVA chemically adsorbed on the surface.

Table 2. The atomic ratio of oxygen and phosphor to silver in Ag_3PO_4 measured using XPS

Sample	O/Ag	P/Ag
Ag_3PO_4	1.61	0.536
Ag_3PO_4/PVA	1.04	0.333

Acknowledgement

This research was supported by the JASSO (Japan Student Services Organization) program of the Follow-up Research Fellowship and the International Research Collaboration Scheme of Republic of Indonesia.

References

[1] Khojasteh, H., Salavati-Niasari, M., Abbasi, A., Azizi, F., Enhessari, M. (2016). Synthesis, Characterization and Photocatalytic Activity of PdO/TiO_2 and Pd/TiO_2 Nanocomposites. *Journal of Materials Science: Materials in Electronics*, 27(2): 1261-1269.

[2] Yang, Z.Y., Shen, G.Y., He, Y.P., Liu, X.X., Yang, S.J. (2016). Preparation of TiO_2/SiO_2 Composite Oxide and its Photocatalytic Degradation of Rhodamine B. *Journal of Porous Materials*, 23(3): 589-599.

[3] Natarajan, K., Kureshy, R.I., Bajaj, H.C., Tayade, R.J. (2016). Photocatalytic Degradation of Indigo Carmine Dye Using Hydrothermally Synthesized Anatase TiO_2 Nanotubes under Ultraviolet Light Emitting Diode Irradiation. *Materials Science Forum*, 855: 45-57.

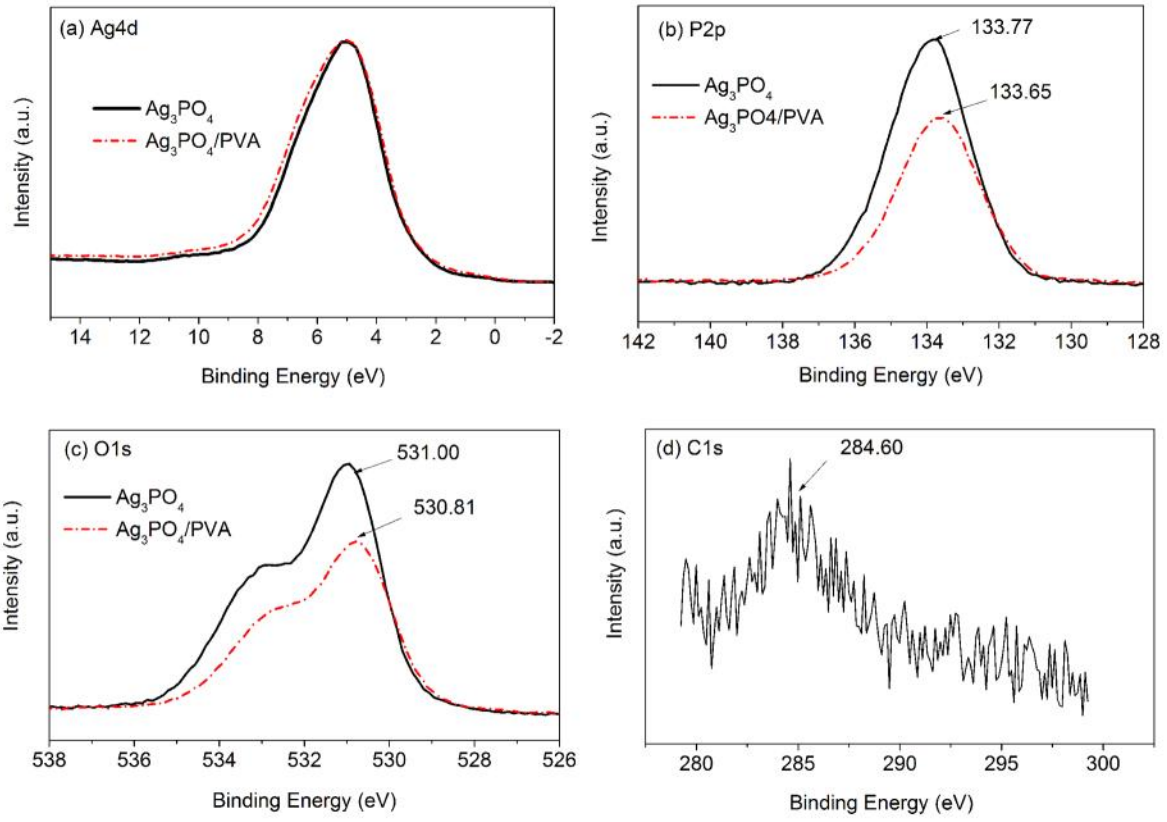

Figure 5. XPS of Ag_3PO_4 and Ag_3PO_4 synthesized using polyvinyl alcohol (Ag_3PO_4/PVA): Ag4d (a), P2p (b), O1s (c) and C1s of Ag_3PO_4/PVA (d). The Ar^+ sputtering is operated to eliminate the compound adsorbed on the surface before analysis

[4] Wu, M., Ouyang, Y., Zhao, K., Ma, Y., Wang, M., Liu, D., Su, Y., Jin, P. (2016). A Novel Fabrication Method for Titanium Dioxide/Activated Carbon Fiber Electrodes and the Effects of Titanium Dioxide on Phenol Degradation. *Journal of Environmental Chemical Engineering*, 4 (3): 3646-3653.

[5] Yi, Z., Ye, J., Kikugawa, N., Kako, T., Ouyang, S., Stuart-Williams, H., Yang, H., Cao, J., Luo, W., Li, Z., Liu, Y., Withers, R.L. (2010). An Orthophosphate Semiconductor with Photooxidation Properties under Visible-Light Irradiation. *Nature Materials*, 9: 559-564.

[6] Sulaeman, U., Nisa, I.R., Riapanitra, A., Iswanto, P., Yin, S., Sato, T. (2014). The Highly Active Photocatalyst of Silver Orthophosphate under Visible Light Irradiation for Phenol Decomposition. *Advanced Materials Research*, 896:141-144.

[7] Hua, X., Jin, Y., Wang, K., Li, N., Liu, H., Chen, M., Paul, S., Zhang, Y., Zhao, X., Teng, F. (2014). Porous Ag_3PO_4 Microtubes with Improved Photocatalytic Properties. *Catalysis Communications*, 52: 49-52.

[8] Yang, Z., Tian, Y., Huang, G., Huang, W., Liu, Y., Jiao, C., Wan, Z., Yan, X., Pan, A. (2014). Novel 3D Fower-like Ag_3PO_4 Microspheres with Highly Enhanced Visible Light Photocatalytic Activity. *Materials Letters*, 116: 209--211.

[9] Yang, Z., Liu, Y., Xu, L., Huang, G., Huang, W. (2014). Facile Shape-Controllable Synthesis of Ag_3PO_4 Photocatalysts. *Materials Letters*, 133: 139-142.

[10] Sulaeman, U., Wu, X., Liu, B., Yin, S., Sato, T. (2015). Synthesis of Ag_3PO_4-Polyvinyl Alcohol Hybrid Microcrystal with Enhanced Visible Light Photocatalytic Activity. *Applied Surface Science*, 356: 226-231.

[11] Sulaeman, U., Febiyanto, F., Yin, S., Sato, T. (2016). The Highly Active Saddle-Like Ag_3PO_4 Photocatalyst Under Visible Light Irradiation. *Catalysis Communications*, 85: 22-25.

[12] Cao, J., Luo, B., Lin, H., Xu, B., Chen, S. (2012). Thermodecomposition Synthesis of WO_3/H_2WO_4 Heterostructure with Enhanced Visible Light Photocatalytic Properties. *Applied Catalysis B: Environmental*, 111-112: 288-296.

[13] Filippo, E., Carlucci, C., Capodilupo, A. L., Perulli, P., Conciauro, F., Corrente, G.A., Gigli, G., Ciccarellaa, G. (2015). Facile Preparation of TiO_2-Polyvinyl Alcohol Hybrid Nanoparticles with Improved Visible Light Photocatalytic Activity. *Applied Surface Science*, 331: 292-298.

[14] Zheng, R., Lin, L., Xie, J., Zhu, Y., Xie, Y. (2008). State of Doped Phosphorus and Its Influence on the Physicochemical and Photocatalytic Properties of P-doped Titania. *The Journal of Physical Chemistry C*, 112 (39): 15502-15509.

[15] Teng, W., Li, X., Zhao, Q., Chen, G. (2013). Fabrication of $Ag/Ag_3PO_4/TiO_2$ Heterostructure Photoelectrodes for Efficient Decomposition of 2-chlorophenol under Visible Light Irradiation. *Journal of Materials Chemistry A*, 1: 9060-9068.

[16] Seo, D., Park, J.C., Song, H. (2006). Polyhedral Gold Nanocrystals with Oh Symmetry: from Octahedra to Cubes. *Journal of the American Chemical Society*, 128(46): 14863-14870.

[17] Chong, R., Cheng, X., Wang, B., Li, D., Chang, Z., Zhang, L. (2016). Enhanced Photocatalytic Activity of Ag_3PO_4 for Oxygen Evolution and Methylene Blue Degeneration: Effect of Calcination Temperature. *International Journal of Hydrogen Energy*, 41(4): 2575-2582.

Selected and Revised Papers from The 2nd International Seminar on Chemistry (ISoC 2016) (Surabaya, 26-27 July 2016) (http://chem.its.ac.id/isoc-2016/) after Peer-reviewed by Scientific Committee of ISoC 2016 and Peer-Reviewers of BCREC journal